Published in final edited form as:

Nature. 2014 February 20; 506(7488): 382–386. doi:10.1038/nature12875.

Selection and evaluation of clinically relevant AAV variants in a xenograft liver model

Leszek Lisowski[1,2], **Allison P. Dane**[3,4], **Kirk Chu**[1], **Yue Zhang**[1], **Sharon C. Cunningham**[3], **Elizabeth M. Wilson**[5], **Sean Nygaard**[6], **Markus Grompe**[6], **Ian E. Alexander**[3,7], and **Mark A. Kay**[1]

[1]Stanford University, School of Medicine, Departments of Pediatrics and Genetics, 269 Campus Drive, Stanford, CA, USA.

[3]Gene Therapy Research Unit, The Children's Hospital at Westmead and Children's Medical Research Institute, Locked Bag 4001, Westmead, NSW, Australia.

[5]Yecuris Corporation, Portland, OR, USA.

[6]Oregon Stem Cell Center, Oregon Health and Science University, Portland, OR, USA.

[7]Discipline of Paediatrics and Child Health, The University of Sydney, NSW, Australia.

Introductory

Recombinant adeno-associated viral (rAAV) vectors show early promise in clinical trials[1–3]. The therapeutic transgene cassette can be packaged in different AAV capsid pseudotypes each having a different transduction profile. Currently, rAAV capsid serotype selection for a

*Corresponding author: Mark A. Kay, 269 Campus Drive, CCSR 2105, Stanford, CA, 94305, USA, Phone: 650-498-6531, Fax: 650-498-6540, markay@stanford.edu.

[2]Currently at: Gene Transfer, Targeting and Therapeutics Core, The Salk Institute for Biological Studies, 10010 N Torrey Pines Rd, San Diego, CA, USA.

[4]Currently at: Department of Haematology, University College London Cancer Institute, London, United Kingdom.

Author Contributions:

Leszek Lisowski – study design, performed experiments and data analysis, prepared figures and the manuscript.
Allison Dane – performed some of the experiments and data analysis, assisted in figure preparation and manuscript editing.
Kirk Chu – helped in performing some of the experiments.
Yue Zhang – performed some of the vector sequence analysis.
Sharon C. Cunningham – performed some of the animal studies, assisted in manuscript editing.
Elizabeth M. Wilson – generated the human transplanted FRG mice in Figure 4c.
Sean Nygaard- injected the animals and prepared tissues for experiment in Figure 4c.
Markus Grompe – helped with establishing FRG colony and provided advice on *in vivo* human hepatocyte repopulation.
Ian E. Alexander - study design and manuscript editing.
Mark A. Kay – study design, manuscript writing and editing.
All the authors reviewed and commented on the manuscript.

Conflict statement:

Oregon Health and Science University (OHSU) and MG have a significant financial interest in YecurisCorp., a company that has some commercial interests in the FRG mouse.
MK has a minor equity stake with stock options value >$5000 and plays no role in the company.
LW is an employee of Yecuris and has no equity.
MG and Yecuris have no ownership or intellectual property rights to any of the new AAV vectors described herein including AAV-LK03.

specific clinical trial is based on effectiveness in animal models. However, preclinical animal studies are not always predictive of the human outcome[4–8]. In an attempt to better understand these discrepancies, we used a chimeric human-murine liver model to directly compare the relative efficiency of rAAV transduction in human vs. mouse hepatocytes *in vivo*. As predicted from preclinical and clinical studies[4,5,8], rAAV2 vectors transduced mouse and human hepatocytes at equivalent but relatively low levels. However, rAAV8 vectors, which are very effective in many animal models, transduced human hepatocytes rather poorly - ~20-times less efficiently than mouse hepatocytes. In light of the limitations of rAAV vectors currently used in clinical studies, we used the same murine chimeric liver model to perform serial selection using a human specific replication competent viral library composed of DNA shuffled AAV capsids. One chimeric capsid composed of 5 different parental AAV capsids was found to transduce human primary hepatocytes at high efficiency *in vitro* and *in vivo*, and provided species-selected transduction in primary liver, cultured cells, and a hepatocellular carcinoma xenograft model. This vector is an ideal clinical candidate and a reagent for gene modification of xenotransplants in mouse models of human diseases. More importantly, our results suggest that humanized murine models may represent a more precise approach for both selecting and evaluating clinically relevant rAAV serotypes for gene therapeutic applications.

Recombinant AAV clinical trials have been hampered by unanticipated immunological responses and lower than expected levels of transgene product[5–8]. For a single serotype there is little correlation between *in vitro* and *in vivo* transduction of primary cells. Between two serotypes, AAV8 and AAV2, the former provides >10-fold higher levels of liver-mediated gene transfer in animals including non-human primates[6,9–11]. An exception may be humans where in the case of hemophilia B[6] the peak level of factor IX transgene product was similar in rAAV2 and rAAV8 treated individuals. There are many potential reasons for the observed discordance in gene transfer efficiency amongst species, but relatively small differences in capsid sequence can affect both cellular uptake and post cell entry processing between species, ultimately affecting the level of gene transfer[12].

In order to establish if murine and human hepatocytes contained within the context of an intact liver are themselves differentially transduced, we injected Fah$^{-/-}$/Rag2$^{-/-}$/Il2rg$^{-/-}$(FRG) mice[13] partially repopulated with primary human hepatocytes (hFRG) with single-stranded or self-complementary rAAV2 and rAAV8 vectors expressing eGFP (Fig. 1a–b). rAAV2 administration resulted in a low but equal number of eGFP positive mouse and human hepatocytes. However, rAAV8 vector resulted in a ~20-fold higher transduction efficiency in mouse compared to human hepatocytes consistent with differences observed in preclinical and clinical studies published to date[6–8,10,11]. The block to functional rAAV8 transduction in human cells was not due to a lack of viral binding/uptake in the human hepatocytes because vector genomes were near equal in both human and mouse hepatocytes by quantitative PCR after laser capture microscopy (LCM) (Fig. 1c). In contrast, the rAAV2 vector genomes were preferentially taken up by human hepatocytes even though gene expression was similar in both the mouse and human cells. These results strongly suggest that differential functional transduction (measured as transgene expression) between capsid serotypes and species can be dependent on post-uptake factors.

Many different approaches have been used to alter the viral capsid and hence the vector transduction properties[14–21]. As our goal was to identify new capsids with improved human tissue transduction, we created and screened a replicating AAV capsid library in the humanized mouse liver model. Our library screens are different from most in that the selection is dependent not only on viral uptake and internalization, but also on viral replication allowing one to select for these important post-uptake parameters that can affect vector-mediated gene transfer (reviewed in [22]).

Ten AAV capsid genes (from AAV1,2,3B[23],4,5,6,8,9, Avian- and Bovine-AAV) were used to generate an AAV shuffled library (see Methods). To perform virus selection *in vivo* we used FRG mice partially repopulated with primary human hepatocytes (see Methods). Because the AAV libraries co-infected with wild-type hAd5 do not replicate in mice[14] we have a stringent simultaneous positive and negative selection between the human and murine cells, respectively.

We performed four rounds of selection (Fig. 2a) and monitored the progress by sequencing >100 clones after each round (Fig. 2b). Library selection in non-humanized FRG animals in the presence of hAd5 served as a negative control and confirmed that rescued AAV was derived from the human cells (Fig. 2b), while a non-humanized FRG animal injected with hAd5 only served as a control to ensure that AAV Cap specific PCR signals were not caused by wt/rAAV contamination of the hAd5 preparation(Fig. 2a–b). After 4 rounds, the three most frequent variants, AAV-LK01, LK02, and LK03 accounted for 22.7%, 4.54%, and 2.3% of the isolates, respectively. From the 19 most abundant variants, rAAV-RSV-eGFP vector preparations of 15 were produced (Fig. 2c). Reconstruction of the genealogical relationship at the DNA and amino acid level between the isolates and parental AAVs used to generate the library is shown in Figure 2d.

We compared the *in vitro* transduction of these 15 AAV vector variants against standard AAV serotypes on a variety of cell types from different species (Extended Data Table 1). In comparison to rAAV-DJ, which efficiently transduces most mouse and human cells in culture[14], rAAV-LK03 preferentially transduced human cells, suggesting that this variant has species-restricted specificity. Importantly, LK03 transduced primary human hepatocytes 100-fold better than AAV8. AAV-LK03 is closely related to AAV3B (Figs.2d and 3a, Extended Data Table 2, Supplementary Table 1, Supplementary Figs. 1 and 2), with lesser contributions from AAV1,2, 4, 6, 8, and 9. rAAV-LK03 transduced human hepatocytes in culture 3, 67, and 6.5-times more than rAAV-DJ rAAV8, and rAAV3B, respectively (Fig. 3b).

A second isolate, AAV-LK19 differed from AAV-LK03 by a single amino acid, S262C. This isolate transduced mouse cell lines and was less efficient than rAAV-LK03 at transducing most human cells with the exception of primary human keratinocytes, where AAV-LK19 resulted in 5 and 7.6-times higher levels compared to rAAV-LK03 and rAAV6, the serotype reported to transduce human keratinocytes[24], respectively (Extended Data Table 1).

Since pre-existing humoral immunity can block the clinical efficacy of a vector[8], we tested selected AAVs in a pooled human IgG (IVIG) neutralization assay (Extended Data Fig. 1 and Methods). Compared to AAV2, AAV3B, AAV-LK03 and AAV-LK19 were much more resistant to IVIG neutralization (Figure 3c), suggesting that these vectors could transduce a large population of humans if used in a clinical trial[25,26].

Due to the similarity between AAV-LK03, -LK19 and AAV3 we wanted to establish if human hepatocyte growth factor (HGF) receptor c-met, previously identified as the AAV3 co-receptor[27], was involved in AAV-LK03 and -LK19 transduction. Transduction of Huh-7 cells with rAAV-hPGK-GFP-P2A-Luc2 in the presence of increasing concentrations of human HGF(hHGF)(used for HGF-R competition) demonstrated that rAAV-LK03, but not rAAV-LK19, was influenced by hHGF (Fig. 3d). These results suggest that the single amino acid difference (S262C) changes the receptor/co-receptor entry of AAV-LK19. While AAV capsid structure is available for several serotypes, the bulk of the sequence variation in these two new pseudotypes were in VP1 (amino acids 1–125), the one region of the capsid for which the structure has yet to be determined, making it difficult to speculate on specific structure/functional relationships.

To compare the relative effectiveness of selected AAVs for transgene expression *in vivo*, we selected eight serotypes to package the hFIX expression cassette used in therAAV2-FIX clinical trial[8]. In mice, the rAAV-LK03 and rAAV-LK19 vectors expressed very low levels of hFIX (Fig. 3e). In contrast, rAAV-LK01 and rAAV-LK02, which are closely related to AAV8/9, and AAV1/6, respectively (Fig. 2d), provided similar levels of expression as that observed with rAAV-DJ and rAAV8. Liver vector copy number (VCN) analysis performed 54 days post vector administration (Extended Data Fig. 2a) correlated with the hFIX expression data, rAAV8>rAAV-LK02~rAAV-DJ>>>rAAV-LK03. Furthermore, liver AAV VCN determined at an early time point (Extended Data Fig. 2b) also correlated with transgene expression (Extended Data Fig. 2c) suggesting that rAAV-LK03 did not enter murine hepatocytes and/or was rapidly degraded upon cell entry.

To further verify the strong species preference, we tested rAAV-LK03, in a hepatocellular carcinoma xenograft model[28]. Animals injected with rAAV3B showed no Luc expression in the liver or tumor, while animals injected with rAAV8 showed Luc expression from the tumor and the liver (Fig. 4a and Supplementary Figs. 3 and 4). Consistent with the data obtained with rAAV-hFIX in normal mice (Fig. 3e and Extended Data Fig. 2c), animals treated with rAAVLK03-RSV-Luc did not show detectable Luc signal from the livers but only from human tumors. In addition, the onset of transgene expression from AAV-LK03 was slower by about 48 hours compared to AAV8 (Extended Data Fig. 3).

Having demonstrated that AAV-LK03 selectively transduced human cells, we next evaluated its transduction efficiency in FRG mice with and without human hepatocyte reconstitution (Fig. 4b). In agreement with previously published data[27], rAAV3B did not transduce murine hepatocytes (control animals in Fig. 4b and Extended Data Fig. 4). Surprisingly rAAV3B, previously shown to transduce human hepatocytes in culture (Ref [27] and Fig 3b), did not lead to detectable Luc expression in engrafted human hepatocytes in this *in vivo* model. In contrast, a strong Luc signal was detected in non-humanized FRG

animals injected with rAAV8-RSV-Luc (Fig. 4b and Extended Data Fig. 4), which efficiently transduced mouse hepatocytes *in vivo* (Fig. 3e and Extended Data Fig. 2). Most importantly, as predicted, the Luc signal was detected in humanized FRG mice injected with rAAV-LK03, but not in non-humanized FRG controls. This data showed that rAAV-LK03 selectively transduces human hepatocytes *in vivo*.

To further quantify the transduction efficiency of rAAV-LK03, we injected an equal dose of rAAV-LK03 or rAAV8-eGFP into humanized FRG mice. One week later, the number of transduced cells was compared (Fig. 4c). The fraction of GFP positive human hepatocytes was 43.3±11% and 3.6±1.1% with LK03 and AAV8 vector infusion, respectively. In contrast, almost all (>99%) mouse hepatocytes were eGFP positive with rAAV8, while <<1% of mouse hepatocytes were eGFP positive after LK03 vector infusion. Thus LK03 transduction measured by the number of transgene positive cells was about 10 times higher than AAV8 in human hepatocytes *in vivo*. This experiment may underestimate the differences in AAV-mediated human hepatocyte transduction because of the variation in the rate of capsid uncoating and peak transgene expression amongst different serotypes. While rAAV8 is rapidly uncoated[29], longer uncoating for rAAV-LK03 can be implied from the slower rise in transgene expression in the tumor xenotransplant transduction studies (Extended Data Fig. 4).

The fact that there was not always a correlation between vector uptake and transgene expression between species (Fig. 1) strongly suggests that post-receptor/entry factors (such as intracellular transport, nuclear entry and/or uncoating) influence the final level of functional transduction (reviewed in [12]). By making replication in human cells a condition for selection, we placed pressure for many of these post-entry parameters. Moreover, the human primary hepatocytes are in an environment emulating their native setting and maintain a more physiological gene expression profile, compared to an *in vitro* setting. This made it more likely to select a candidate that will be useful in humans. A summary of the transduction efficiencies of standard and newly selected AAV capsids described here is shown in Extended Data Table 3. Taken together, the rAAV-LK03 based vector is not only a highly promising clinical candidate, but will also prove useful when restricted genetic manipulation of xenotransplanted cells/tissues is required.

Most importantly, our studies suggest that the use of a human primary cell xenotransplant model compared to commonly used mouse and NHP models may more accurately predict the potential transduction efficiency in humans. The approach provided herein may accelerate the ability to identify and establish clinically useful AAV vector candidates for clinical trials where current serotype selection is in large part based on gene transfer efficiency in animal models.

Methods

AAV Library generation

The AAV library was generated as previously described[14] with minor modifications. AAV capsid genes (*cap*) from AAV 1, 2, 3, 4, 5, 6, 8, 9, Avian-AAV and Bovine-AAV were PCR amplified and cloned into TOPO® PCR Cloning Kit (Life Technologies, Grand Island, NY)

and sequenced. Cap genes were cut out using PacI and AscI, mixed at 1:1 ratio and digested using DNaseI (Roche) for 1, 5, 10, 15, 20, 25, and 30 min. All reactions were separated on 1%(w/v) agarose gel, and fragments <1000 bp were cut out and used in a primerless PCR reassembly step, followed by a second round of PCR including primers binding outside the Cap gene (Forward Primer 5'-GTC TGAGTGACTAGCATTCG and Reverse Primer 5'-GCTTACTGAAGCTCACTGAG)[14]. Final reassembled shuffled Cap genes were cloned into the AAV recipient plasmid based on wtAAV2. The final ligations were transformed into 40 independent competent DH5α cell aliquots and plated on 100 15 cm LB/agar plates. 100 clones were picked and sequenced to confirm library variability. The remaining clones were scraped, pooled and expanded in liquid LB+Amp culture. Final library plasmid DNA was extracted using EndoFree Megaprep Kit (Qiagen) and used for AAV library production.

AAV vectors and AAV library production

AAV library and AAV vectors were packaged as previously described using a $Ca_3(PO_4)_2$ transfection protocol, followed by CsCl gradient purification as described[14]. Vectors used in studies shown in Figure 1 and 4c were tittered by quantitative PCRas described[30], while all other vectors used in the study were titrated by quantitative dot blot as described[32]. All AAV productions were performed using HEK293 cells (ATCC, Cat# CRL-1573). AAV library yielded a preparation with a particle titer of 2×10^{12}vg/mL.

Humanized FRG animals

Animal housing and all animal work was performed in accordance to the ethical guidelines for animal care at Stanford University and the CMRI and CHW Animal Care and Ethics Committee. $Fah^{-/-}/Rag2^{-/-}/Il2rg^{-/-}$(FRG)[13] breeding pairs (M. Grompe lab, OHSU) were used to establish FRG mouse colonies at Stanford University and the CMRI. In order to restrict the variability due to the host cells, all mice used during library selection were transplanted with fresh hepatocytes obtained from a single donor, a 52-year-old Caucasian female with neuroendocrine tumor without chemotherapy treatment. Mice used in studies shown in Figure 1a and 4a were transplanted with cryopreserved primary hepatocytes (isolated by collagenase perfusion from pediatric donors or purchased from Invitrogen(Cat# HMCPIS, Lot# Hu8089) (1×10^6 viable cells per mouse) as described[13]. This mouse model has been used for testing other specific human processes related to drug metabolism and infectious diseases[33].

For studies shown in Figure 2a and 4b, only 8–12 weeks old female mice were used for repopulation, while for studies shown in Figure 1 and 4c, both repopulated males and females were used. 24hrs prior to hepatocyte transplantation, mice received *i.v.* injection of 5×10^{10} p.f.u. of human urokinase (uPA) adenoviral vector[34]. Each animal received 1×10^6 hepatocyte via intrasplenic injection. Mice received subcutaneous injections of IL2R blocker (1.5 mg/animal/day) – Kineret (Anakinra) for 7 days. NTBC cycles were initiated 48 hrs after transplantations, as described[13].

The progress of liver repopulation was monitored by biweekly human albumin ELISA using Human Albumin ELISA Quantitation Kit (Bethyl Labs, Cat# E88-129) and goat anti-human albumin HRP antibody (crossed adsorbed against bovine, mouse, pig) (Bethyl Labs, Cat#

A80-229P, Lot # A80-229P-13) as per the manufacturer's instructions, with 1 mg/mL hAlb being equivalent to ~20% repopulation. Engrafted hepatocytes were allowed to expand before mice were transduced with rAAV; vector was injected 73–124 days post-transplant (with a mean of 96 days post-transplant). Human hepatocyte transplanted mice containing at least 5% human hepatocytes (for studies shown in Fig 2a) or at least 40% (for studies in Fig 1a and 4b–c) were placed into separate cages with number tags. At the time of vector administration, the available mice were randomly picked out of the cage and treated sequentially with the various viruses/vector treatment groups.

In vivo AAV Library selection, AAV Cap PCR and AAV variant vectorization

FRG animals received 1×10^{11}vg/animal AAV library via *i.v.* injection followed by *i.v.* injection of wild type human Ad5 (VR-5 - ATCC) 24 hrs later. Livers were harvested 48 hrs after hAd5 injection, minced and frozen in aliquots in liquid nitrogen. One aliquot was used for AAV purification. Sample was mixed with 2× volume PBS per weight (200 μL PBS per 100 μg tissue) and underwent 3 freeze/thaw cycles followed by tissue homogenization, hAd5 inactivation (65°C for 30 min), and 5 min spin at 14,000×g at 4°C. The clear supernatant was used for subsequent *in vivo* selection step and PCR analysis. For PCR analysis, 1 μL of the supernatant were used for AAV DNA extraction using WAKO DNA Extraction Kit (WAKO, Japan), followed by PCR amplification (Forward: 5'-GATCTGGTCAATGTGGATTTG and Reverse: 5'-ACCGCAGCCTTTCGAATGTCC). PCR was performed using KAPA HiFi HotStart ReadyMix (KAPA Biosystems, Woburn, MA) and following program: 2 min 98°C, 30 cycles of 20 sec 98°C, 15 sec 55°C, 72°C 1 min. 2.3 kb PCR product was cloned into TOPO® PCR Cloning Kit (Life Technologies, Grand Island, NY) and 100+ clones were sent for sequencing. Clones selected for vectorization were PCR amplified using customized oligos: Forward 5'-acATTTAAATCAGGT-**ATG**-N27 and Reverse 5'-GTTTAAACGAATTCGCCCTTCGCAGAGACCAAAGTTCAACTGAAACGAATCAACCGGTTTATTGATTAACAGGCAA-**TTA**-N27 (Start and Stop codons of Cap are shown in bold and N27 represents 27 nt following ATG or preceding TTA for given AAV clone), cloned into TOPO cloning kit, verified, released using AscI-PacI digestion and cloned in frame downstream of Rep into predigested recipient pCap plasmid containing AAV2 Rep without ITR sequences. The variability of the final library was confirmed by sequencing one hundred random clones and demonstrating that each clone had a unique sequence with extensive genetic diversity.

Shuffled Vector Sequence analysis

AAV Cap sequences obtained from TOPO cloning were analyzed using Geneious 6.0.5 software (Biomatters Ltd, New Zealand). Geneious was used for DNA and protein sequence alignments and for reconstruction of the genealogical relationship among viral isolates.

Shuffled AAV sequence contribution analysis

An in-house Perl pipeline was set up to analyze the results of sequence alignment by the NCBI BLAST suite (blastn and blastp). The pipeline generated the overall serotype

composition of novel AAVs by comparison of DNA and amino acid sequences with their parent AAVs based on maximum likelihood.

In vitro transduction analysis and transduction titer calculation

Cells were plated in 24 well tissue culture coated plates in appropriate media 16hrs prior to transduction. Cells were transduced with AAV-RSV-GFP vectors at four 10-fold dilutions for 16 hrs. GFP levels were analyzed using Fluorescence-activated cell sorting (FACS) using BD LSR II. The percentage of GFP^+ cells was used to calculate transduction titer [TU/mL] by using the following formula: TU/mL = (%GFP/100)*(cell number at transduction)*(dilution factor). Transduction titer was normalized to dot blot titer [vg/mL]. For each cell line, the vector with the lowest normalized transduction [TU/vg] was assigned the value 1 and used as a basis for normalization of all other vectors.

Primary Human Hepatocytes culture and transduction

Fresh primary human hepatocytes were plated on plates coated with rat tail Collagen Type II (BD Biosciences) in HMM Hepatocyte Maintenance Medium with UltraGlutamin-1 (Lonza). Cells were transduced with AAV-RSV-Luc (Extended Data Table 1) or rAAV-PGK-GFP-P2A-Luc2-pA (Figure 3b) vectors for 16 hrs. For experiment shown in Figure 3b cells were transduced at the same MOI based on Dot Blot titer. 72 hrs after transduction, cells were washed in PBS and analyzed using Dual-Luciferase Assay System (Promega) and Tecan M-1000 luminometer.

Mycoplasma testing

All cell lines and primary cells used in the study underwent mycoplasma testing prior to use. Negative mycoplasma contamination status was verified using LookOut Mycoplasma PCR Kit (Sigma, Cat# MP0035) and MycoAlert Mycoplasma Detection Kit + Assay Control (Lonza, Cat# LT07-318 and LT07-518).

IVIG neutralization assay

IVIG neutralization assay was adopted, with modifications, from Arbetman*et al*.[31] Two Intravenous immunoglobulin (IVIG) preparations, Gammagard S/D (Baxter/Hyland; Deerfield, Ill) (IgA content of 1.6 μg/mL in 5% solution) and Gamunex (Bayer) (IgA content of 46 mcg/mL), were initially compared side by side using Huh-7 cells (generous gift from Dr. Jeff Glenn, Stanford University). rAAV2-RSV-Luc2 vector was used as a positive control to establish IVIG neutralization assay. Two protocols were compared. AAV pre-incubation with IVIG at 4°C overnight and 37°C for 60 min. As shown in Extended Data Fig. 1, both preparations showed similar profile of AAV2 neutralization. For all future experiments, 60 min AAV pre-incubation with IVIG at 37°C was used.

For rAAV variants IVIG neutralization assay, identical number of vector particles of the 8 selected rAAV variants were incubated with increasing concentrations of Gammagard/ Gamunex at 37°C prior to Huh7 cell transduction in DMEM media without FBS. Cells were washed 5hrs later and allowed to grow for 72 hrs in DMEM+10%FBS(v/v). Cell were harvested and analyzed for Luc expression (see above).

hHGF competition assay

Human hepatocyte growth factor competition assay was performed as in Ling *et al*[27]. Huh7 cells were transduced with rAAV-PGK-GFP-P2A-Luc2 at MOI 2×10^4. Vectors were premixed with increasing concentrations of Recombinant Human Hepatocyte Growth Factor(HGF) (Life Technologies). Cells were analyzed for Luc levels 72 hrs after transduction (see above).

In vivo hFIX expression and analysis

6 to 8 weeks old female C57BL/6 mice (Jackson Laboratory, Bar Harbor, ME) received retro-orbital (r.o.) injection of 5×10^{10}vg rAAV-hFIX-16 vectors. Blood was collected at the indicated time points *via* r.o. bleeding, and plasma hFIX levels were determined via an enzyme-linked immunosorbent assay (ELISA) as described [35].

In Vivo vector copy number (VCN) analysis

Genomic DNA was extracted from indicated tissues using DNeasy Blood & Tissue Kit (Qiagen) according to manufacturer's instructions. Multiplex real-time TaqMan PCR was performed on BioRad CFX384 using:

hFIX-probe	5'-6FAM-CCACATGGAAATGGCACTGCTGGT
hFIX-forward-primer	5'-GTACTGAGGGATATCGACTTGC
hFIX-reverse-primer	5'-GCACGGGTGAGCTTAGAAGTTTGT
β-actin probe	5'-VIC-GCTGTGTTCTTGCACTCCTTGCATGT
β-actin forward-primer	5'-TGAGACTCCCAGCACACTGAACTT
β-actin reverse-primer	5'-ACACTCAGGGCAGGTGAAACTGTA

In vivo Luc assay

For *in vivo* Luc imaging, animals received *i.v*. injections of 5×10^{10}vg (FRG mice, Figure 4b) or 1×10^{11}vg (NOD/SCID mice, Figure 4a) of AAV-RSV-Luc variants. Naïve animals injected with the same doses of rAAV vectors served as controls. Animals were imaged every 48 hrs using Xenogen IVIS Lumina imaging system (Caliper Lifesciences, Hopkinton, MA) after intraperitoneal injection of D-luciferin substrate(120 mg/kg). Living Image software was used for bioluminescent image analysis. Detailed analysis of images shown in Fig 4a and 4b, including region of interest(ROI) quantification (Total Flux [p/s] and Average Radiance [p/s/cm2/sr]) is shown in Extended Data Figure 3, Extended Data Figure 4, Supplementary Figure 3, and Supplementary Figures 4.

Analysis of vector genome copy number in mouse and human hepatocytes populations using laser capture microscopy (LCM) and QPCR

Liver sections from engrafted mice transduced with rAAV, and harvested 2 weeks later, were immunostained for human albumin as described above. The PALM MicroBeam System (Carl Zeiss GmbH, Germany) was used to collect areas of mouse and human hepatocytes. All the clusters of human cells in 2 to 4 0.5μm liver sections per mouse, and 2

to 4 samples of mouse hepatocyte areas (roughly equivalent to the area of human cells collected) were collected by laser capture microscopy. Samples were collected into 30 μL digestion buffer (10 mM Tris pH8.3, 50 mM KCl, 1.5 mM $MgCl_2$, 0.5% (v/v) Tween 20) and incubated overnight at 56°C with 20 μg/mL Proteinase K (Roche) which was inactivated at 96°C for 10 min. Vector genome content was determined by QPCR on 5 μL of lysed sample, with no further purification, using primers and probe to the WPRE (single-stranded vectors) or eGFP (self-complementary vectors) as described for viral titering. The reactions were carried out on 5 μL of sample or standards (plasmid or human/mouse genomic DNA). To account for potential cross contamination of samples with cells from the other species, and to normalize for sample size, human and mouse GAPDH QPCR was performed on each sample. Reactions using 2× QuantiTect®Sybr® Green Master mix (Qiagen) and 0.5 μM forward primer (for mouse GAPDH 5' ACGGCAAATTCAACGGCAC; for human GAPDH 5' GCTCTCTGCTCCTCCTGTTCG) and 0.5 μM reverse primer (for mouse GAPDH 5' TAGTGGGGTCTCGCTCCTGG; for human GAPDH 5' GCGAACACATCCGGCCTGC). Standards consisted of genomic DNA prepared from mouse NIH3T3 cells or human HEK 293 cells (100–0.0625 ng/reaction). Total GAPDH per LCM sample was determined and therefore the proportion of the sample that was human (or mouse) calculated. The vector genome amount was adjusted accordingly and normalized.

Hepatocellular carcinomas xenograft model

Hepatocellular carcinoma xenograft model was established as describe[28], with modifications. 6–8 weeks old female NOD/SCID mice were obtained from Jackson Laboratory (Bar Harbor, ME). Mice were gamma-irradiated at 3Gy 24hrs prior to cell transplantation. Mice received subcutaneous injection of Huh7 cells on the dorsal side of the neck between shoulder blades. 1×10^6 Huh7 cells mixed 1:1 with matrigel (BD Biosciences) were injected in 200uL total. Animals were kept in separate sterile cages until the end of the experiment.

Immunohistochemistry, microscopy, image processing and fluorescent cells counts

In order to avoid any bias, all samples were blinded prior to immunohistochemical analysis, so that the person processing the samples did not know what vectors were used to inject given animals. Only after the final samples were analyzed and described, were the samples unblended and matched to vectors used.

For the detection of human albumin, human FAH and eGFPas shown in Figure 1 and Figure 4c, hFRG mice with human albumin levels between 1.2–3.2mg/mL (equivalent to ~24–64% repopulation) were injected with 5×10^{10}vg (Figure 1) or 5×10^{11}vg (Figure 4c) of rAAV-LSP1.eGFP[30]. Tissues were harvested 10–14days post AAV administration and livers were fixed in 4% (w/v) PFA after harvest and processed through a sucrose gradient (10 to 30% w/v) before freezing in Optimum Cutting Temperature (O.C.T; Tissue-Tek, Sakura Finetek USA, Torrance CA) freezing media. Frozen liver sections (5μm) were permeabilised in ice-cold methanol, blocked with 13% (v/v) donkey serum (Sigma) and 8.7% (v/v) FBS in PBS −/−, then reacted with a goat polyclonal anti-human albumin primary antibody (1/200 dilution; Bethyl Labs, Cat # A80 299P) or a rabbit polyclonal anti-FAH primary antibody (1/200 dilution; Sigma-Aldrich, Cat # AV41681). Primary antibody was detected with either

an Alexa Fluor 594 donkey anti-goat IgG secondary antibody (1/1000 dilution; Invitrogen, Carlsbad, CA, Cat # A11058) or an Alexa Fluor 594 donkey anti-rabbit IgG secondary antibody (1/800 dilution; Invitrogen, Carlsbad, CA, Cat # A21207). After immunolabelling sections were analysed on an Olympus BX51 upright microscope using filter sets D350/50x (excitation) and D460/50m (emission) for DAPI fluorescence; D480/30x (excitation) and D535/40m (emission) for eGFP fluorescence; HQ560/55 (excitation) and HQ645/75 (emission) for Alexa Fluor 594 fluorescence. Images were captured was a Spot Enhancer black and white digital camera using Spot Version 4.0 imaging program (Diagnostic Instruments, Sterling Heights, MI) and merged to determine co-localisation of eGFP and human albumin.

The percentage of transduced human hepatocytes per field of view was determined by individually analyzing and comparing images taken using filters D480/30x (excitation) and D535/40m (emission) and HQ560/55 (excitation) and HQ645/75 (emission) to detect eGFP fluorescence and FAH immunostaining (Alexa 594), respectively, rather than direct analysis of merged images. The latter gives an underestimate due to variability of eGFP fluorescence intensity in individual hepatocytes.

Statistical Analyses

Statistical analysis shown in Figure 3b was done using one-way ANOVA with Sidak's multiple comparison test using GraphPad Prism 6 software.

Supplementary Material

Refer to Web version on PubMed Central for supplementary material.

Acknowledgments

This work was supported by: M.A.K NIH HL092096, HL064274. Leszek Lisowski was supported in part by the Berry Fellowship Foundation. I.E.A. NHMRC 1008021

References

1. Bainbridge JW, et al. Effect of gene therapy on visual function in Leber's congenital amaurosis. N Engl J Med. 2008; 358:2231–2239. [PubMed: 18441371]
2. Gaudet D, et al. Efficacy and long-term safety of alipogene tiparvovec (AAV1-LPL(S447X)) gene therapy for lipoprotein lipase deficiency: an open-label trial. Gene Ther. 2012
3. Bennett J, et al. AAV2 gene therapy readministration in three adults with congenital blindness. Science translational medicine. 2012; 4:120ra115.
4. Nietupski JB, et al. Systemic administration of AAV8-alpha-galactosidase A induces humoral tolerance in nonhuman primates despite low hepatic expression. Mol Ther. 2011; 19:1999–2011. [PubMed: 21712814]
5. Jiang H, et al. Effects of transient immunosuppression on adenoassociated, virus-mediated, liver-directed gene transfer in rhesus macaques and implications for human gene therapy. Blood. 2006; 108:3321–3328. [PubMed: 16868252]
6. Nathwani AC, et al. Adenovirus-associated virus vector-mediated gene transfer in hemophilia B. N Engl J Med. 2011; 365:2357–2365. [PubMed: 22149959]
7. Kay MA, et al. Evidence for gene transfer and expression of factor IX in haemophilia B patients treated with an AAV vector. Nature genetics. 2000; 24:257–261. [PubMed: 10700178]

8. Manno CS, et al. Successful transduction of liver in hemophilia by AAV-Factor IX and limitations imposed by the host immune response. Nat Med. 2006; 12:342–347. doi:nm1358 [pii]10.1038/nm1358. [PubMed: 16474400]
9. Nathwani AC, et al. Safe and efficient transduction of the liver after peripheral vein infusion of self-complementary AAV vector results in stable therapeutic expression of human FIX in nonhuman primates. Blood. 2007; 109:1414–1421. [PubMed: 17090654]
10. Nathwani AC, et al. Self-complementary adeno-associated virus vectors containing a novel liver-specific human factor IX expression cassette enable highly efficient transduction of murine and nonhuman primate liver. Blood. 2006; 107:2653–2661. [PubMed: 16322469]
11. Davidoff AM, et al. Comparison of the ability of adeno-associated viral vectors pseudotyped with serotype 2, 5, and 8 capsid proteins to mediate efficient transduction of the liver in murine and nonhuman primate models. Mol Ther. 2005; 11:875–888. [PubMed: 15922958]
12. Nonnenmacher M, Weber T. Intracellular transport of recombinant adeno-associated virus vectors. Gene Ther. 2012; 19:649–658. [PubMed: 22357511]
13. Azuma H, et al. Robust expansion of human hepatocytes in Fah−/−/Rag2−/−/Il2rg−/− mice. Nat Biotechnol. 2007; 25:903–910. doi:nbt1326 [pii]10.1038/nbt1326. [PubMed: 17664939]
14. Grimm D, et al. In vitro and in vivo gene therapy vector evolution via multispecies interbreeding and retargeting of adeno-associated viruses. J Virol. 2008; 82:5887–5911. doi:JVI.00254-08 [pii]10.1128/JVI.00254-08. [PubMed: 18400866]
15. Muller OJ, et al. Random peptide libraries displayed on adeno-associated virus to select for targeted gene therapy vectors. Nat Biotechnol. 2003; 21:1040–1046. [PubMed: 12897791]
16. Perabo L, et al. In vitro selection of viral vectors with modified tropism: the adeno-associated virus display. Mol Ther. 2003; 8:151–157. [PubMed: 12842438]
17. Maheshri N, Koerber JT, Kaspar BK, Schaffer DV. Directed evolution of adeno-associated virus yields enhanced gene delivery vectors. Nat Biotechnol. 2006; 24:198–204. [PubMed: 16429148]
18. Li W, et al. Engineering and selection of shuffled AAV genomes: a new strategy for producing targeted biological nanoparticles. Mol Ther. 2008; 16:1252–1260. [PubMed: 18500254]
19. Pulicherla N, et al. Engineering liver-detargeted AAV9 vectors for cardiac and musculoskeletal gene transfer. Mol Ther. 2011; 19:1070–1078. [PubMed: 21364538]
20. Asuri P, et al. Directed evolution of adeno-associated virus for enhanced gene delivery and gene targeting in human pluripotent stem cells. Mol Ther. 2012; 20:329–338. [PubMed: 22108859]
21. Yang L, et al. A myocardium tropic adeno-associated virus (AAV) evolved by DNA shuffling and in vivo selection. Proceedings of the National Academy of Sciences of the United States of America. 2009; 106:3946–3951. [PubMed: 19234115]
22. Choi VW, McCarty DM, Samulski RJ. AAV hybrid serotypes: improved vectors for gene delivery. Current gene therapy. 2005; 5:299–310. [PubMed: 15975007]
23. Rutledge EA, Halbert CL, Russell DW. Infectious clones and vectors derived from adeno-associated virus (AAV) serotypes other than AAV type 2. J Virol. 1998; 72:309–319. [PubMed: 9420229]
24. Petek LM, Fleckman P, Miller DG. Efficient KRT14 targeting and functional characterization of transplanted human keratinocytes for the treatment of epidermolysis bullosa simplex. Mol Ther. 2010; 18:1624–1632. [PubMed: 20571545]
25. Calcedo R, Vandenberghe LH, Gao G, Lin J, Wilson JM. Worldwide epidemiology of neutralizing antibodies to adeno-associated viruses. The Journal of infectious diseases. 2009; 199:381–390. [PubMed: 19133809]
26. Boutin S, et al. Prevalence of serum IgG and neutralizing factors against adeno-associated virus (AAV) types 1, 2, 5, 6, 8, and 9 in the healthy population: implications for gene therapy using AAV vectors. Hum Gene Ther. 2010; 21:704–712. [PubMed: 20095819]
27. Ling C, et al. Human hepatocyte growth factor receptor is a cellular coreceptor for adeno-associated virus serotype 3. Hum Gene Ther. 2010; 21:1741–1747. [PubMed: 20545554]
28. Hazari S, et al. Hepatocellular carcinoma xenograft supports HCV replication: a mouse model for evaluating antivirals. World journal of gastroenterology : WJG. 2011; 17:300–312. [PubMed: 21253388]

29. Thomas CE, Storm TA, Huang Z, Kay MA. Rapid uncoating of vector genomes is the key to efficient liver transduction with pseudotyped adeno-associated virus vectors. J Virol. 2004; 78:3110–3122. [PubMed: 14990730]

30. Cunningham SC, Dane AP, Spinoulas A, Logan GJ, Alexander IE. Gene delivery to the juvenile mouse liver using AAV2/8 vectors. Mol Ther. 2008; 16:1081–1088. [PubMed: 18414478]

Additional References

31. Arbetman AE, et al. Novel caprine adeno-associated virus (AAV) capsid (AAV-Go.1) is closely related to the primate AAV-5 and has unique tropism and neutralization properties. J Virol. 2005; 79:15238–15245. [PubMed: 16306595]

32. Nakai H, et al. A limited number of transducible hepatocytes restricts a wide-range linear vector dose response in recombinant adeno-associated virus-mediated liver transduction. J Virol. 2002; 76:11343–11349. [PubMed: 12388694]

33. Grompe M, Strom S. Mice with human livers. Gastroenterology. 2013

34. Lieber A, Peeters MJ, Gown A, Perkins J, Kay MA. A modified urokinase plasminogen activator induces liver regeneration without bleeding. Hum Gene Ther. 1995; 6:1029–1037. [PubMed: 7578415]

35. Lisowski L, et al. Ribosomal DNA integrating rAAV-rDNA vectors allow for stable transgene expression. Mol Ther. 2012; 20:1912–1923. [PubMed: 22990671]

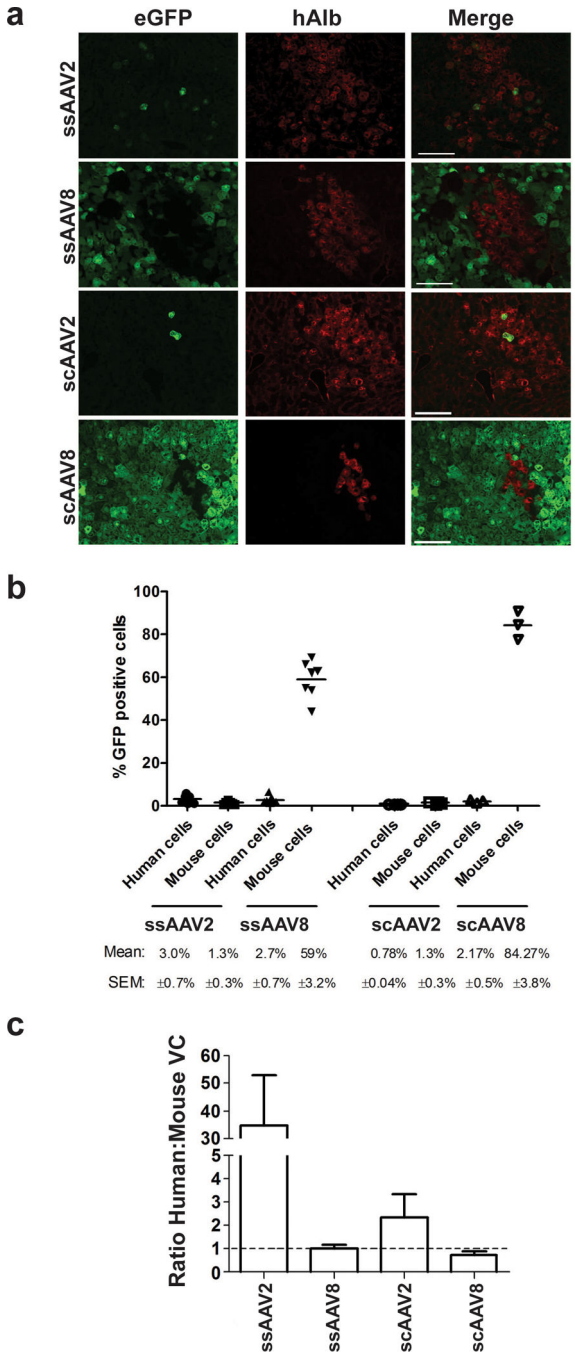

Figure 1.

In vivo comparison between rAAV2 and rAAV8. (**a**) Representative histological images from the humanized FRG mouse livers transduced with 5×10^{10}vg single-stranded (ss) and self-complementary (sc) rAAV2 and rAAV8. hAlb – human Albumin. Scale bar = 100μm. The percentage of transduced human hepatocytes was determined by individually analyzing and comparing cell counts from images of eGFP fluorescence and FAH immunostaining (see methods for details). (**b**) Quantification of data shown in (a). For ssAAV2 and ssAAV8 groups n=7/each; for scAAV2 n=4, for scAAV8 n=3, up to 10 sections per mouse were

scored. **(c)** Ratio of vector genomes in human *vs.* mouse hepatocytes *in vivo*. Laser capture microdissection (LCM) followed by QPCR analysis was use to obtain relative vector copy (VC) numbers in each population (see Methods), error bars=SD, n=3.

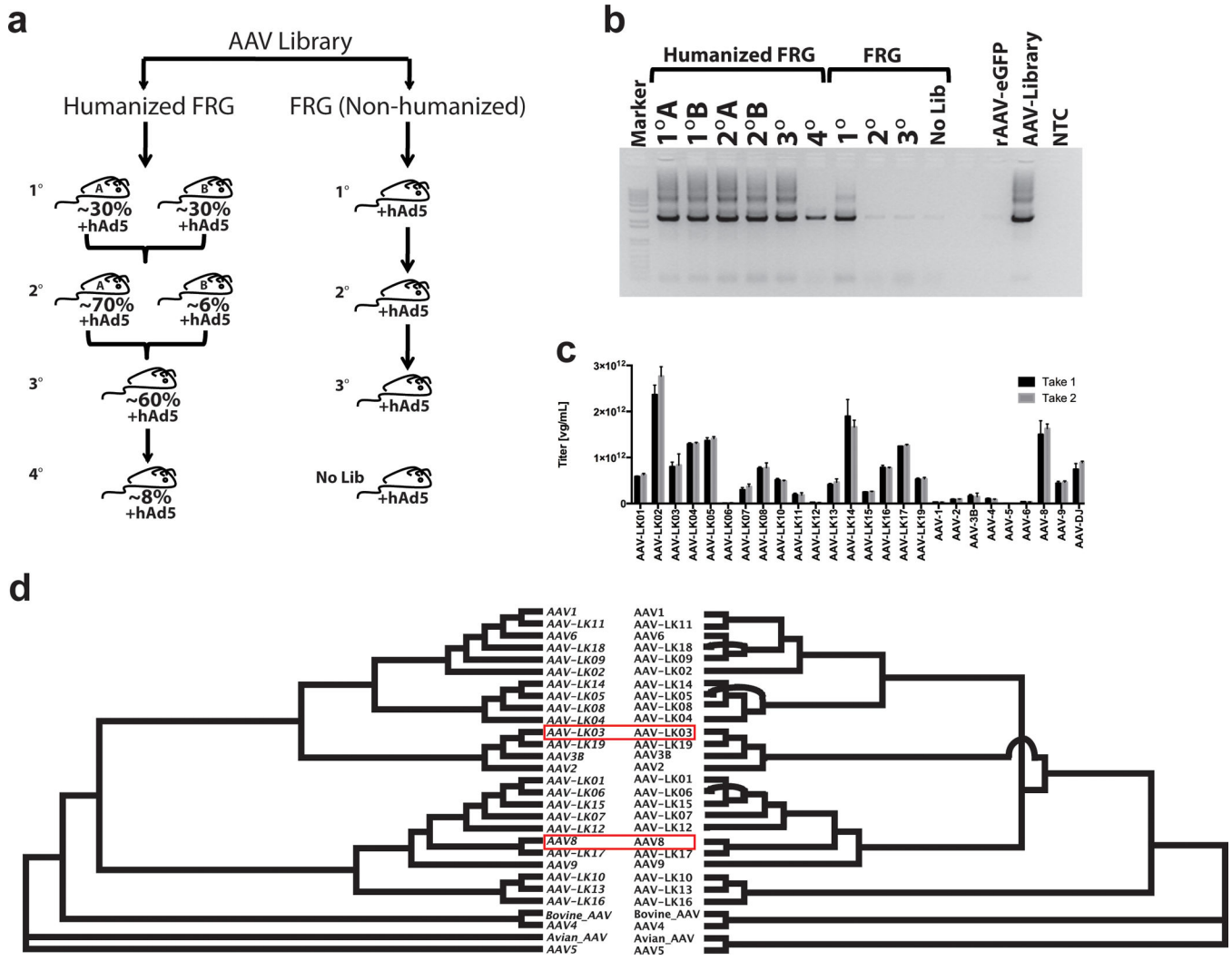

Figure 2.

In vivo AAV shuffled library screen. (**a**) Graphic representation of the screen. N=2 passage 1&2, n=1 passage 3&4. Percentage of human hepatocyte repopulation is listed. Selection was performed once (single biological repeat). (**b**) PCR analysis of liver lysates after each selection step. NTC–no template control. Marker–1kb+ DNA ladder. (**c**) Dot blot titer comparison between parental AAVs, AAV-DJ, and novel isolates for two transduction experiments, error bars=SD, n=3. (**d**) Genealogical relationship of isolates at protein (left panel) and DNA (right panel) levels.

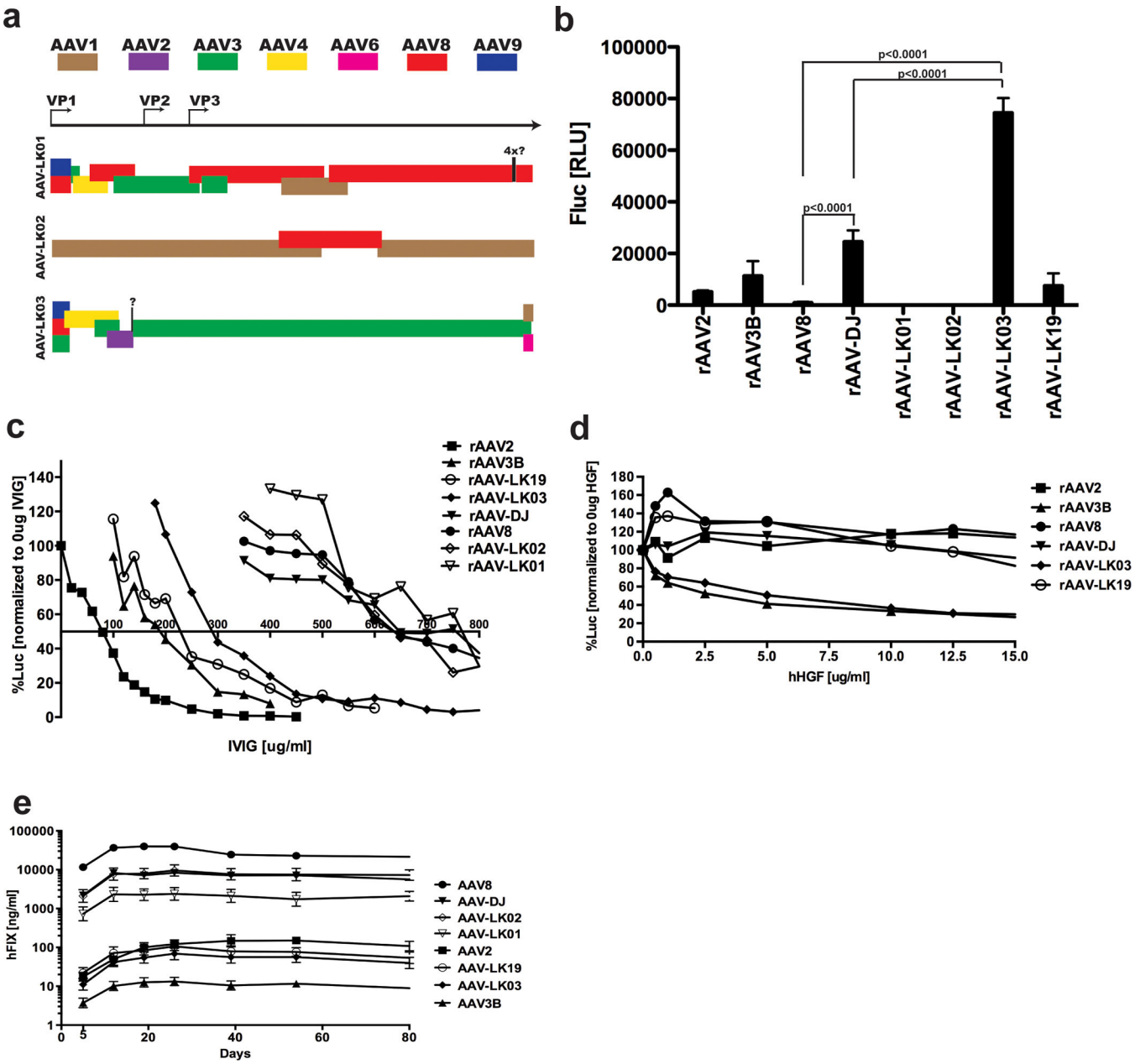

Figure 3.

Functional analysis of selected isolates. (**a**) Contribution comparison for the top 3 isolates in graphic form. Residues with unknown parental origin are indicated as "?". (**b**) Transgene expression in primary human hepatocytes in culture (see Methods). Error bars represent SD, n=4 from a single biological repeat. (**c**) Intravenous immunoglobulin (IVIG) neutralization assay, n=4 (<15% variation). (**d**) Human hepatocyte growth factor competition assay. Data represents averages from two biological repeats with n=3 per repeat. (**e**) Comparison of hFIX expression in C57BL6 mice. N=5 animals/group up to day 54, n=2 at day 80. Single biological repeat, also see Extended Data Fig. 2c.

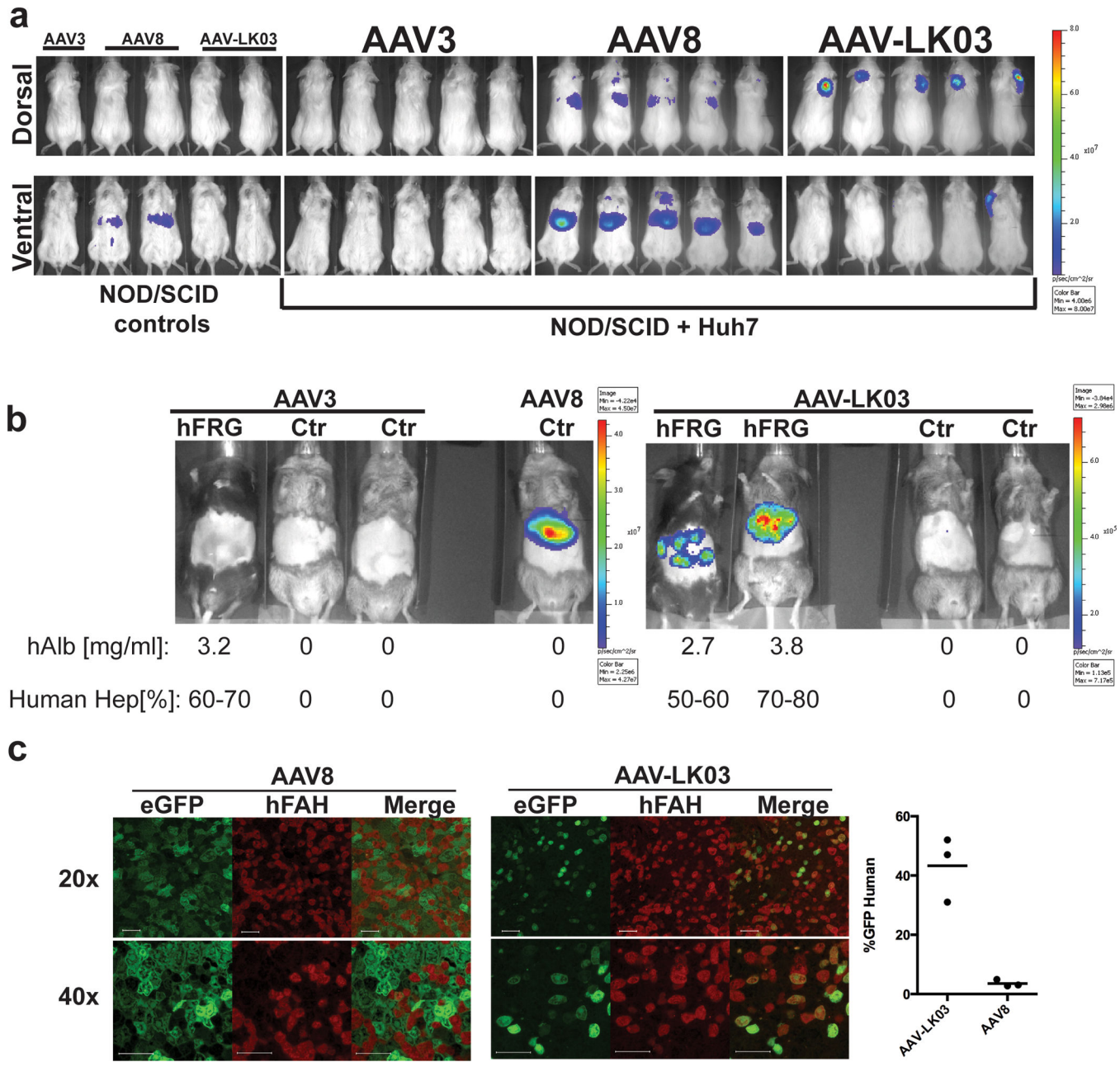

Figure 4.

In vivo vector specificity analysis. (**a**) Luc expression in human hepatocellular carcinoma xenograft model 6 days after *i.v.* vector injection (n=5/group). Controls = naïve animals. The same results were observed in two independent biological repeats. (**b**) Luc expression in humanized FRG animals (hFRG) or naïve controls (Ctr). Serum human albumin (hAlb) levels and estimated percentages of human hepatocyte repopulation are given. All animals used in the study are shown – n=1+2 (rAAV3), n=1 (rAAV8), n=2+2 (rAAV-LK03) (**c**) *In vivo* comparisons between hFRG animals transduced with 5×10^{11}vg rAAV8 or rAAV-LK03. Representative histological images are shown. Cell counting was as in Fig. 1a and

detailed in the methods. hFAH–human fumarylacetoacetate hydrolase. Scale bar = 100μm. The graph represents quantification of *in vivo* data from 3 animals.